Nuclear Instruments and Methods in Physics Research A 1080 (2025) 170704

Contents lists available at ScienceDirect

Nuclear Inst. and Methods in Physics Research, A

journal homepage: www.elsevier.com/locate/nima

X-ray irradiation studies on the Monopix DMAPS in 150 nm and 180 nm

Christian Bespin [a,*], Marlon Barbero [b], Pierre Barrillon [b], Patrick Breugnon [b], Ivan Caicedo [a], Yavuz Degerli [c], Jochen Dingfelder [a], Tomasz Hemperek [a,1], Toko Hirono [a,2], Hans Krüger [a], Fabian Hügging [a], Konstantinos Moustakas [a,3], Patrick Pangaud [b], Heinz Pernegger [d], Petra Riedler [d], Piotr Rymaszewski [a,1], Lars Schall [a,*], Philippe Schwemling [c], Walter Snoeys [d], Tianyang Wang [a,4], Norbert Wermes [a], Sinou Zhang [a]

[a] Physikalisches Institut der Universität Bonn, Nußallee 12, 53115, Bonn, Germany
[b] CPPM, Aix Marseille Université, 163 Avenue de Luminy, 13288, Marseille, France
[c] IRFU, Bâtiment 141, 91191, Gif-sur-Yvette, France
[d] CERN, Espl. des Particules 1, 1217, Geneva, Switzerland

ARTICLE INFO

Keywords:
Pixel detector
Monolithic
Radiation hardness
Monopix

ABSTRACT

Monolithic active pixel sensors with depleted substrates present a promising option for pixel detectors in high-radiation environments. High-resistivity silicon substrates and high bias voltage capabilities in commercial CMOS technologies facilitate depletion of the charge sensitive volume. TJ-Monopix2 and LF-Monopix2 are the most recent large-scale chips in their respective development line, aiming for the ATLAS Inner Tracker outer layer requirements. Those include a tolerance to ionizing radiation of up to 100 Mrad. It was evaluated by irradiating both devices with X-rays to the corresponding ionization dose, showing no significant degradation of the performance at 100 Mrad and continuous operability throughout the irradiation campaign.

1. Introduction

The fabrication of monolithic pixel detectors for high-energy physics experiments in commercial CMOS processes has been successfully demonstrated in many projects and chips in recent years. With the original design specifications to meet the ATLAS Inner Tracker outer pixel layer requirements, the development of LF- and TJ-Monopix was heavily influenced by the expected hit rate and radiation levels in terms of ionizing and non-ionizing radiation.

2. The Monopix2 chips

Both monolithic pixel detector prototypes, LF- and TJ-Monopix2, utilize commercial CMOS imaging technologies with 150 nm and 180 nm feature size, respectively. They are fabricated in highly resistive silicon and employ technologies with high-voltage capabilities to enhance depletion of the charge-sensitive sensor substrate. The pixels are read out using a column-drain mechanism derived from the FE-I3 ATLAS readout chip [1]. Both chips feature time over threshold charge measurements and in-pixel threshold tuning circuitry.

2.1. LF-Monopix2

The LF-Monopix2 chip features 150 × 50 μm large pixels arranged in a matrix of 56×340 pixels. Its large n-well collection electrode houses the analog and digital pixel electronics inside. This design approach offers short drift distances, high and homogeneous electrical fields for fast charge collection, and high NIEL (non-ionizing energy loss) radiation tolerance [2]. It exhibits a detector capacitance in the order of 250 fF which results in a power consumption of about 28 μW/pixel [3]. Fig. 1 shows the schematic cross-section of the pixel design. An elaborated guard ring designs allows for bias voltages above 450 V before irradiation [3].

* Corresponding authors.
E-mail addresses: cbespin@uni-bonn.de (C. Bespin), lars.schall@uni-bonn.de (L. Schall).
[1] Now at DECTRIS AG, Baden-Dättwil, Switzerland.
[2] Now at Karlsruher Institut für Technologie, Karlsruhe, Germany.
[3] Now at Paul Scherrer Institut, Villingen, Switzerland.
[4] Now at Zhangjiang National Laboratory, Pudong, China.

https://doi.org/10.1016/j.nima.2025.170704
Received 17 April 2025; Received in revised form 23 May 2025; Accepted 27 May 2025
Available online 13 June 2025

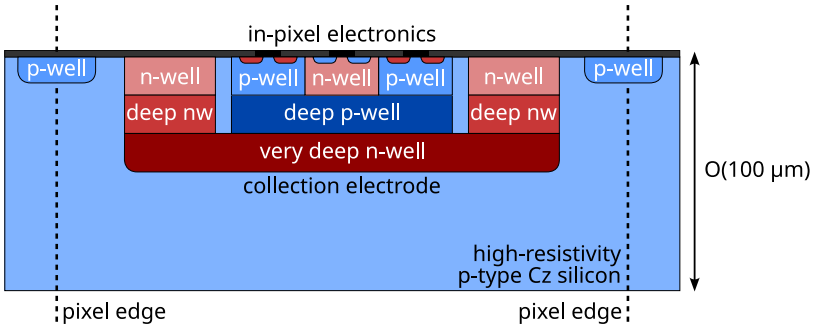

Fig. 1. Schematic cross-section of a pixel in the large collection electrode design of LF-Monopix2.

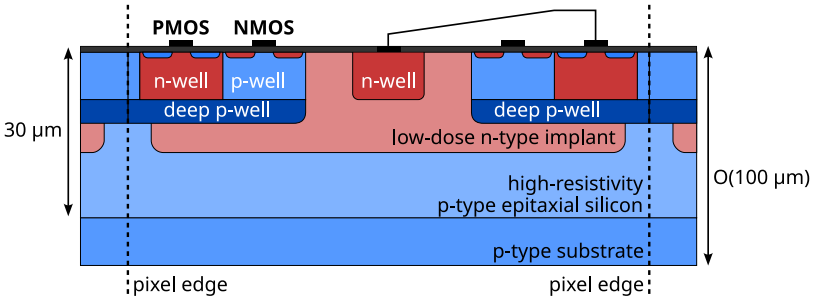

Fig. 2. Schematic cross-section of a pixel in the small collection electrode design of TJ-Monopix2.

2.2. TJ-Monopix2

TJ-Monopix2 is a large-scale chip with a 17 mm×17 mm large matrix composed of square pixels with 33 µm pitch. The pixel electronics are implemented in p-wells that are spatially separated from the small (2 µm diameter) n-type charge collection electrode. This design facilitates a small detector capacitance in the order of 2 fF enabling an analog power consumption of as low as 1 µW/pixel [4]. Due to the longer drift distances and inhomogeneous electrical field compared to the large collection electrode design, further enhancements are necessary to achieve tolerance against NIEL radiation. A low-dose n-type layer close to the top side of the sensor leads to a depletion boundary parallel to the pixel and a more homogeneous depletion of the highly-resistive epitaxial silicon [5]. The cross-section of this geometry is depicted in Fig. 2. The gaps of this n-type implantation at the pixel edges improve the field shape below the p-wells in which the electronics are located [6,7].

3. X-ray irradiation setup and dosimetry

The irradiation campaigns were performed at an X-ray irradiation system with a Tungsten anode at the University of Bonn [8]. Fig. 3 depicts the dose rate profile measured with a silicon diode from which the dose rate during the irradiation is extracted. The chips are placed in the central part to maximize the dose rate on the respective device under test. During the irradiation, the devices under test are powered up and cooled to 0 °Celsius by mounting them on a cold plate.

4. Measurement results of LF-Monopix2

Two front-end variants of LF-Monopix2 were studied that have a similar amplifier design, but different gain. Fig. 4 depicts the gain of the tested front-ends with their respective feedback capacitance against the deposited dose. No significant change can be observed over the full dose range which is in agreement with earlier measurements on this amplifier design [9]. The same study finds that the feedback current in this amplifier design is also unaffected.

Monitoring the different power domains of LF-Monopix2 (for the analog and digital pixel electronics, and the end-of-column logic) enables to investigate the X-ray dose influence on the different circuitry within the chip. The corresponding graphs are presented in Fig. 5. While the current consumption of the end-of-column logic is unaffected, the current consumption of the analog circuits decreases from 1 Mrad on to about 50 % of its initial value. The digital circuitry exhibits a decrease between 100 krad and 1 Mrad and increases to almost twice of its initial value between 1 Mrad and 10 Mrad It follows the behavior of the analog power domain at higher dose levels. This increase has been observed for NMOS transistors of a comparable feature size in multiple studies. The stated underlying reasons are two-fold [10,11]:

Hole accumulation Radiation-induced positive charges get trapped in the silicon oxide and introduce a threshold voltage shift that is proportional to the amount of trapped charges and depends on the distance thereof to the Si-SiO_2 interface.

Interface traps For NMOS transistors, negative charges are trapped in so-called interface traps and counteract the aforementioned threshold voltage shift.

Since the analog part uses well-shielded NMOS transistors, only the effect of interface traps can be observed for higher doses. The threshold shift of the NMOS transistors in the digital circuitry increases their leakage current and, consequently, the current consumption.

An influence on the operation can be observed in the threshold dispersion that shows an increase of about a factor of four at 100 Mrad compared to the non-irradiated state. This dispersion limits the operational threshold since pixels at the lower end of the distribution exhibit thresholds below the noise level. The in-pixel threshold tuning in LF-Monopix2 enables compensation of the threshold variations across the matrix and limits the threshold dispersion to an increase of up to 25 % over the measured dose range, resulting in the same operational threshold of 1980 e^- at 100 Mrad compared to 2050 e^- at 0 Mrad.

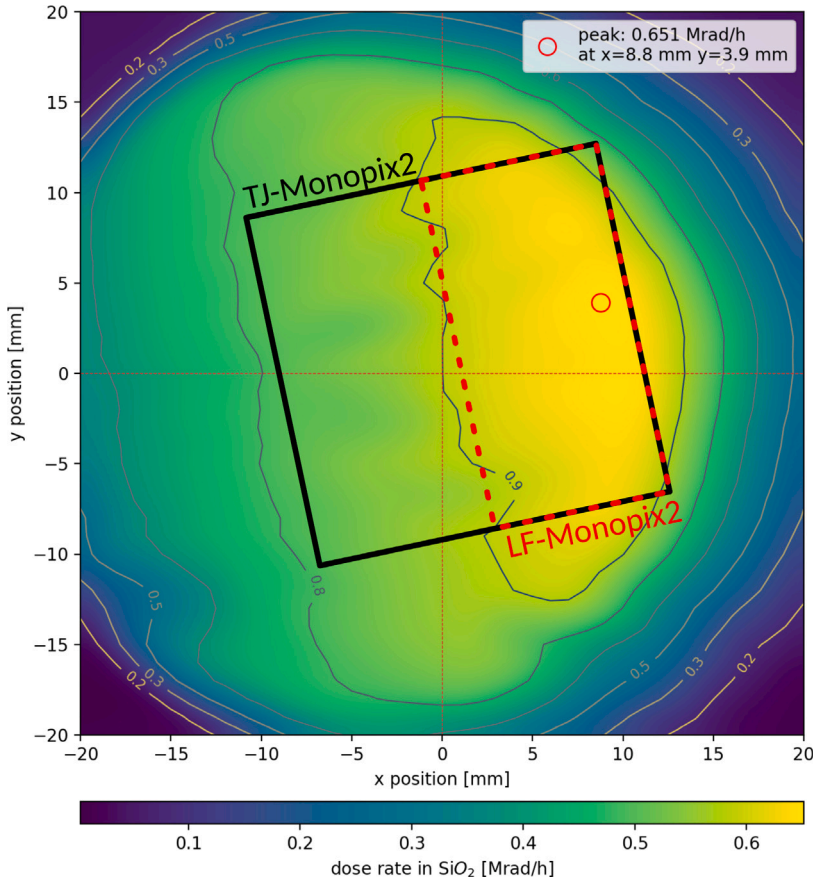

Fig. 3. Dose rate map of the irradiation setup, measured with a silicon diode. The positions of the TJ- and LF-Monopix2 devices under test are depicted by the black and red rectangles, respectively.

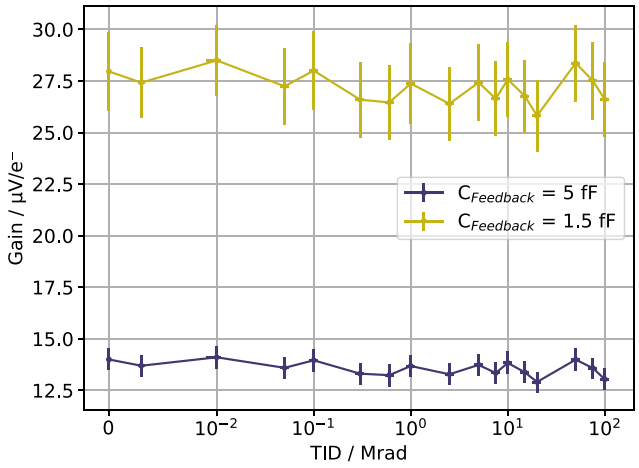

Fig. 4. Evolution of the gain of LF-Monopix2 versus total ionization dose for two front-ends that differ in their feedback capacitance. For both, the gain does not degrade over the whole dose range.

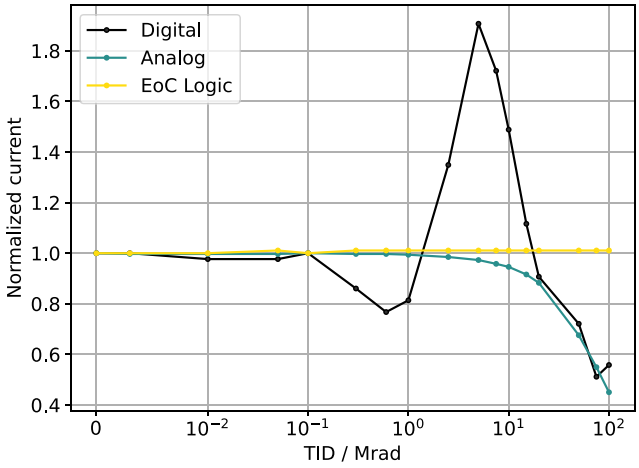

Fig. 5. Normalized current consumption (at 1.8 V) of the different power domains of LF-Monopix2 versus the ionization dose.

5. Measurement results of TJ-Monopix2

The power consumption of TJ-Monopix2 versus the total irradiation dose, depicted in Fig. 6 exhibits a similar behavior as in LF-Monopix2, originating from the same effects. Since the voltage amplifier input transistor is implemented as an NMOS device, a significant degradation of the gain has been observed in the expected dose range between 1 Mrad and 10 Mrad. This conclusion is supported by measuring the baseline after the amplifier stage that shows the same decrease in the aforementioned dose range. As in LF-Monopix2, the threshold dispersion increases, but can be counter-acted by utilizing the in-pixel threshold tuning capabilities. This facilitates an operational threshold of 245 e^- after 100 Mrad which is an increase of only 15 e^- of the threshold in the non-irradiated chip.

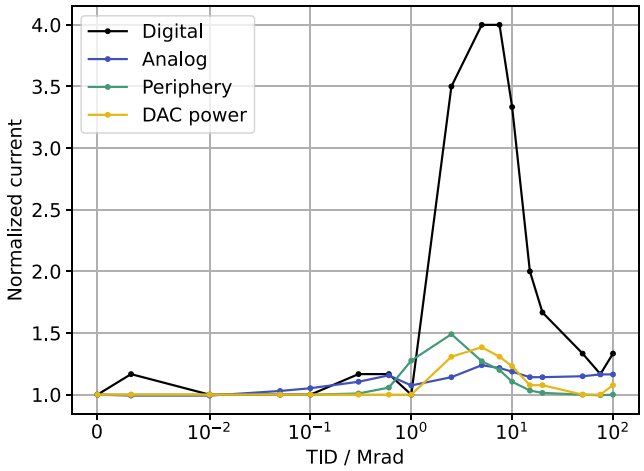

Fig. 6. Normalized current consumption (at 1.8 V) of the different power domains of TJ-Monopix2 versus the ionization dose.

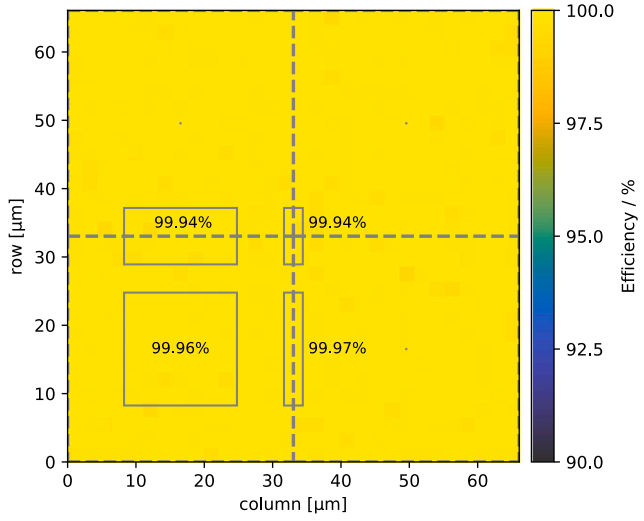

Fig. 7. In-pixel efficiency map of TJ-Monopix2 after X-ray irradiation to 100 Mrad.

Table 1
Summary table of achieved performance of LF-Monopix2 and TJ-Monopix2 at 0 Mrad and 100 Mrad irradiation dose.

	LF-Monopix2		TJ-Monopix2	
	0 Mrad	100 Mrad	0 Mrad	100 Mrad
Thr./e^-	2055	1983	230	254
Thr. disp./e^-	91	108	5	5
ENC/e^-	92	112	6	13

5.1. Beam tests

Furthermore, the irradiated sensor has been measured in a beam test campaign at the DESY II test beam facility [12]. The device has been cooled to 0 °Celsius as during the irradiation and presented measurements. The hit detection efficiency has been evaluated to 99.94(5) % which is consistent with the efficiency of 99.96 % before irradiation [13]. Fig. 7 shows the homogeneous in-pixel efficiency map after a total dose of 100 Mrad with individual values for different pixel regions. In addition, the time resolution of about 1 ns before irradiation is matched [14].

6. Conclusion

Both DMAPS were successfully X-ray irradiated to 100 Mrad and remained fully functional at the highest dose level. The power consumption follows the characteristic and, therefore, expected course for NMOS transistors of the respective feature size. By utilizing the in-pixel threshold tuning capabilities and adjusting the front-end settings, the overall performance shows no significant degradation. The threshold, threshold dispersion, and equivalent noise charge (ENC) before and after irradiation are summarized in Table 1.

Declaration of competing interest

The authors declare that they have no known competing financial interests or personal relationships that could have appeared to influence the work reported in this paper.

Acknowledgments

Parts of the measurements have been performed at the Test Beam Facility at DESY Hamburg (Germany), a member of the Helmholtz Association (HGF). This project has received funding from the European Union's Horizon 2020 Research and Innovation programme under the Marie-Sklodowska-Curie GA No. 675587 (STREAM), under GA No. 654168 (AIDA-2020), and GA No. 101004761 (AIDAinnova).

References

[1] I. Perić, et al., The FEI3 readout chip for the ATLAS pixel detector, Nucl. Instrum. Methods Phys. Res. Sect. A Accel. Spectrometers Detect. Assoc. Equip. 565 (1) (2006) 178–187, http://dx.doi.org/10.1016/j.nima.2006.05.032, Proceedings of the International Workshop on Semiconductor Pixel Detectors for Particles and Imaging.
[2] L. Schall, et al., Test-beam performance of proton-irradiated, large-scale depleted monolithic active pixel sensors in 150 nm CMOS technology, in: Proceedings of the 32nd International Workshop on Vertex Detectors (VERTEX2023), vol. 448, 2024, p. 043, http://dx.doi.org/10.22323/1.448.0043.
[3] I. Caicedo, et al., Improvement in the Design and Performance of the Monopix2 Reticle-Scale DMAPS, in: JPS Conference Proceedings, vol. 42, http://dx.doi.org/10.7566/JPSCP.42.011021, 202.
[4] K. Moustakas, Design and Development of Depleted Monolithic Active Pixel Sensors with Small Collection Electrode for High-Radiation Applications (Ph.D. thesis), Rheinische Friedrich-Wilhelms-Universität Bonn, 2021.
[5] W. Snoeys, et al., A process modification for CMOS monolithic active pixel sensors for enhanced depletion, timing performance and radiation tolerance, Nucl. Instrum. Methods Phys. Res. Sect. A Accel. Spectrometers Detect. Assoc. Equip. 871 (2017) 90–96, http://dx.doi.org/10.1016/j.nima.2017.07.046.
[6] M. Munker, et al., Simulations of CMOS pixel sensors with a small collection electrode, improved for a faster charge collection and increased radiation tolerance, J. Instrum. 14 (05) (2019) C05013, http://dx.doi.org/10.1088/1748-0221/14/05/C05013.
[7] M. Dyndal, et al., Mini-MALTA: radiation hard pixel designs for small-electrode monolithic CMOS sensors for the high luminosity LHC, J. Instrum. 15 (02) (2020) P02005, http://dx.doi.org/10.1088/1748-0221/15/02/P02005.
[8] A. Qamesh, X-ray Irradiation and Calibration of the RD53A Pixel Read-out Chip (Master's thesis), Rheinische Friedrich-Wilhelms-Universität Bonn, 2019.
[9] T. Hirono, Development of depleted monolithic active pixel sensors for high rate and high radiation experiments at HL-LHC (Ph.D. thesis), 2019–03, Rheinische Friedrich-Wilhelms-Universität Bonn, 2019.
[10] F. Faccio, G. Cervelli, Radiation-induced edge effects in deep submicron CMOS transistors, IEEE Trans. Nucl. Sci. 52 (6) (2005) 2413–2420, http://dx.doi.org/10.1109/TNS.2005.860698.
[11] L. Gonella, et al., Total ionizing dose effects in 130-nm commercial CMOS technologies for HEP experiments, Nucl. Instrum. Methods Phys. Res. Sect. A Accel. Spectrometers Detect. Assoc. Equip. 582 (3) (2007) 750–754, http://dx.doi.org/10.1016/j.nima.2007.07.068, VERTEX 2006.
[12] R. Diener, et al., The DESY II test beam facility, Nucl. Instrum. Methods Phys. Res. Sect. A Accel. Spectrometers Detect. Assoc. Equip. 922 (2019) 265–286, http://dx.doi.org/10.1016/j.nima.2018.11.133.
[13] C. Bespin, Characterization of the TJ-Monopix2 Depleted Monolithic Active Pixel Sensor for High-Energy Physics Experiments (Ph.D. thesis), Rheinische Friedrich-Wilhelms-Universität Bonn, 2024, http://dx.doi.org/10.48565/bonndoc-427.
[14] C. Bespin, et al., Timing performance of a monolithic CMOS pixel detector front-end in 180nm technology, in: 2024 Panhellenic Conference on Electronics & Telecommunications, PACET, IEEE, 2024, pp. 1–4, http://dx.doi.org/10.1109/PACET60398.2024.10497069.